Nano-Elastohydrodynamics: Structure, Dynamics, and Flow in Nonuniform Lubricated Junctions

Jianping Gao, W. D. Luedtke, Uzi Landman*

Structure, flow, and response characteristics of molecularly thin films of hexadecane, sheared by topographically nonuniform solid gold surfaces sliding at a relative velocity of 10 meters per second, were investigated with molecular dynamics simulations. The simulations reveal three characteristics: spatial and temporal variations in the density and pressure of the lubricant in the region confined by the approaching asperities, accompanied by asperity-induced molecular layering transitions that are reflected in oscillatory patterns in the friction force; asperity deformations and microstructural transformations mediated by the lubricant; and an onset of cavitated zones in the lubricant after the asperity-asperity collision process. The simulations extend micrometer-scale elastohydrodynamic investigations into the nanometer-scale regime and provide molecular-scale insights into the fundamental mechanisms of ultrathin film lubrication phenomena under extreme conditions.

The general purposes of a lubricating fluid are to provide a protective coating to the solid surfaces, thus preventing formation of adhesive junctions, and to reduce frictional energy losses by acting as an interfacial layer of low shear strength (*1–3*). Underlying the development in the early 1960s of the theory of elastohydrodynamic lubrication (EHL) (*3, 4*) was the observation that when two nonconforming solid surfaces come into contact in the presence of a liquid lubricant (or when two asperities of nominally conforming surfaces, under conditions of boundary lubrication, come together), the pressure developed in the contact zone may achieve such high values that local elastic deformations of the surfaces must be included in proper treatments of lubrication of the tribosystem. The subsequent development of micrometer-scale EHL (micro-EHL) and numerical algorithms (*3, 4*) allowed investigators to focus on lubrication processes involving individual surface irregularities (asperities) and has aided the design of machine elements and bio-tribological systems (*5, 6*) of improved efficiency and durability. Inherent to these continuum models are certain assumptions that are used as input into the calculations. These include constitutive relations such as rheological properties of the lubricant film (Newtonian or non-Newtonian viscosity laws, as well as pressure and temperature variations of the viscosity) and mechanical response characteristics of the bounding surface materials (substrates and asperities), as well as imposed interfacial liquid-solid boundary conditions.

The ever-increasing trend toward miniaturization of technological devices and the ability to fabricate such structures, coupled with the emergence and proliferation of proximal probes (in particular, tip-based microscopies and the surface force apparatus) and of atomic-scale simulation techniques, provide the impetus and the means for nanometer-scale modifications and manipulations of materials and allow systematic investigations of interfacial problems of fundamental and technological interest with unprecedented high spatial and temporal resolutions and under extreme conditions (*7, 8*). Through such investigations it was found that molecular structure and dynamics, mechanical response, and rheology at interfaces and in confined thin films are often very different from those in the bulk and cannot be understood by simple extrapolation of bulk properties (*7*). However, even though the surfaces of even the most highly polished engineering components are characterized by roughness on a broad range of length scales (*9*), most recent work, using atomic-force and friction-force microscopies, the surface force apparatus (SFA), and molecular dynamics (MD) simulations, focused on atomically structured flat and smooth confining surfaces (*7*).

Asperity-asperity collisions, formation and subsequent breakage of interfacial adhesive junctions, and shear-induced rheological transformations in highly confined fluids are among the most fundamental processes in tribology as well as boundary and thin-film lubrication (*1, 7*). To investigate the atomic and molecular origins of such processes in morphologically nonuniform lubricated narrow junctions sheared at high velocities we have used MD simulations (*7, 8*), thus extending micro-EHL investigations to the nanometer-scale regime, is beyond the range of applicability of continuum-based models. In such simulations the equations of motion of a system of particles interacting by means of prescribed interatomic potentials are numerically integrated, and the resulting phase-space trajectories are analyzed. For model systems we used thin films of hexadecane (n-$C_{16}H_{34}$) confined between two gold substrates exposing (111) surfaces [that is, Au(111)]. Topographical nonuniformities (asperities) were modeled by flat-top pyramidal gold structures of height h_a from the underlying gold surface, extending a finite length in the x direction and over the whole simulation cell in the y direction (that is, asperity ridges; see views along the y direction in Fig. 1).

The interactions between the gold atoms were modeled by many-body embedded-atom method interactions (*10*), which provide a proper description of the nature of cohesion in metals. The alkane molecules were simulated by using the united atom model (*11, 12*), with the interaction potentials between the CH_2 and CH_3 segments of the molecules including harmonic intramolecular bond-stretch and bond-angle bending potentials, a dihedral angle potential, and nonbonded intra- and intermolecular interactions. The interactions between the molecular segments and the gold atoms were modeled by 6–12 Lennard-Jones potentials with parameters fitted to experimentally estimated desorption data (*12*). These potentials have been tested and used successfully in previous studies of bulk and interfacial alkane systems (*11–13*).

The Newtonian equations of motion were integrated by using the Verlet algorithm (*14*), with an integration time step $\Delta t = 3.06 \times 10^{-15}$ s; for each of our systems a typical simulation consisted of 4×10^5 Δt, that is, 1.2 ns, past a prolonged equilibration stage. In simulations of shear-induced flow, the solid surfaces were kept at a constant separation (chosen to correspond to an initially vanishing average normal load) and were translated along the x axis in opposite directions, with the top and bottom surfaces moving with a constant velocity of +5 and −5 m/s (a relative sliding velocity V = 10 m/s). In these simulations the alkane molecules and the gold atoms of the asperities were treated dynamically. The simulations were performed isothermally, at a temperature T = 350 K, through scaling of intramolecular velocities in 50 Δt intervals.

To explore the dependence of structure, dynamics, and flow on the characteristics of the lubricated junctions, we studied mainly three lubricated systems. The first consists of 422 hexadecane molecules with the separation between the gold surfaces S = 36.1 Å, the height of each of the asperities h_a = 9.3 Å, and thus the separation between the asperity tops $\Delta h_{aa} = S - 2h_a$ = 17.5 Å; the second system, which we refer to as the near-overlap case, consists of 243 molecules, with S = 23.2 Å, h_a = 9.3 Å, and Δh_{aa} = 4.6 Å; and the third system, referred

School of Physics, Georgia Institute of Technology, Atlanta, GA 30332, USA.

*To whom correspondence should be addressed.

to as the overlap case (see Fig. 1), consists of 201 molecules, with S = 21.3 Å, h_a = 14 Å, and $\Delta h_{aa} = -6.7$ Å. In describing our results we denote by d_{aa} the distance along the x direction between the leading edges of the opposing asperities. For each system the simulations of sliding followed equilibration, with the asperities well distanced from each other, such that steady-state flow could be established before the onset of effects caused by lubricant confinement in the interasperity region.

Atomic and molecular configurations of the three simulated systems, recorded in each case at selected times during the shearing process, are displayed in Fig. 1. The main patterns illustrated by these configurations are (i) the evolution of liquid layered structures in the region between the colliding asperities and (ii) the severe deformations of the asperities for the cases of near-overlapping (Fig. 1B) and overlapping (Fig. 1C) asperity heights. It is particularly noteworthy that although in all cases a certain degree of interfacial layering in the vicinity of the solid boundaries already existed at equilibrium and for large transverse separations between the asperities, the layering of the lubricant in the interasperity region was initially absent and developed dynamically as the asperities approached each other. Furthermore, the number of layers in the interasperity region evolved in each case in a "quantized" manner as successive layers were squeezed out of it when the asperities came closer together.

These atomic and molecular structural variations are portrayed in the behavior of the forces acting between the thin-film molecules and the solid substrates, as well as by the intermetallic interactions between the two solid surfaces. As a demonstration we show in Fig. 2 the time variation of the forces in the shear and normal directions (f_x and f_z, respectively) recorded during a simulation of the near-overlapping system. Of particular interest are the oscillatory patterns in the forces before the collision between the asperities, whose characteristics correlate with the structural layering stages of the lubricating film (compare Figs. 1B and 2; note that the marked minima in f_x and f_z, seen particularly clearly in f_x, correspond to successively decreasing discrete numbers of molecular layers in the interasperity region).

The aspects revealed by our investigations are that molecular density layering and consequent solvation force oscillations can occur not only in liquids confined between smooth solid surfaces under equilibrium conditions (*7*), but also under constant-velocity shear-flow conditions in a lubricated junction with nonuniform surfaces, and that such oscillations, correlated with quantization of the number of lubricant layers in a localized region of the contact (that is, the interasperity zone), can be exhibited both in the normal (f_z) as well as the tangential (f_x) forces. The implication of these observations (which we have made also for the two other simulated systems) is that such oscillations in the force resisting the relative sliding motion (that is, the friction force, f_x) may lead to stick-slip behavior in experiments where the sliding of the substrates (kept at constant normal separation) is driven by means of a connection through a spring element to a stage dragged at constant velocity [as in SFA measurements (*7*, *15*)].

Another aspect revealed by the simulations pertains to the crucial importance of the dynamical mechanical response of the substrates, and in particular that of the irregularities (asperities), in determining the evolution and properties of sheared systems, as is illustrated through the atomic configurations shown in Fig. 1 and the force and local stress plots shown for the near-overlap

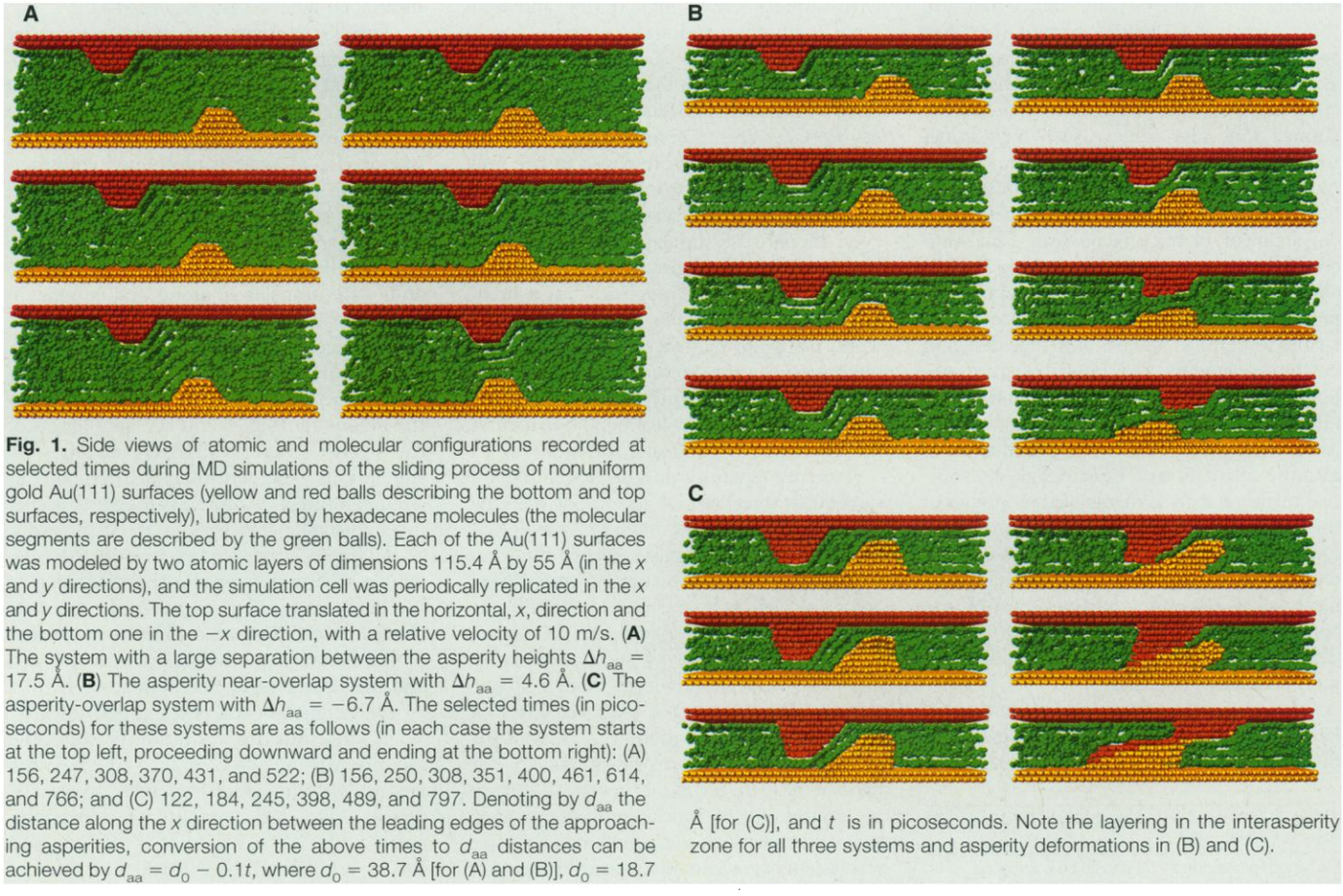

Fig. 1. Side views of atomic and molecular configurations recorded at selected times during MD simulations of the sliding process of nonuniform gold Au(111) surfaces (yellow and red balls describing the bottom and top surfaces, respectively), lubricated by hexadecane molecules (the molecular segments are described by the green balls). Each of the Au(111) surfaces was modeled by two atomic layers of dimensions 115.4 Å by 55 Å (in the x and y directions), and the simulation cell was periodically replicated in the x and y directions. The top surface translated in the horizontal, x, direction and the bottom one in the $-x$ direction, with a relative velocity of 10 m/s. (**A**) The system with a large separation between the asperity heights Δh_{aa} = 17.5 Å. (**B**) The asperity near-overlap system with Δh_{aa} = 4.6 Å. (**C**) The asperity-overlap system with $\Delta h_{aa} = -6.7$ Å. The selected times (in picoseconds) for these systems are as follows (in each case the system starts at the top left, proceeding downward and ending at the bottom right): (A) 156, 247, 308, 370, 431, and 522; (B) 156, 250, 308, 351, 400, 461, 614, and 766; and (C) 122, 184, 245, 398, 489, and 797. Denoting by d_{aa} the distance along the x direction between the leading edges of the approaching asperities, conversion of the above times to d_{aa} distances can be achieved by $d_{aa} = d_0 - 0.1t$, where d_0 = 38.7 Å [for (A) and (B)], d_0 = 18.7 Å [for (C)], and t is in picoseconds. Note the layering in the interasperity zone for all three systems and asperity deformations in (B) and (C).

system in Figs. 2 and 3, respectively. For relatively large spacing between the asperity heights (Δh_{aa} = 17.5 Å, Fig. 1A), shear-flow accompanied by structuring of the lubricant occurs with no distortions of the metal surfaces. However, in the cases of nearly overlapping (Fig. 1B) and overlapping (Fig. 1C) surface irregularities, large densification and pressurization of the lubricant in the interasperity region occur, accompanied by a significant increase of the effective viscosity in that region [detailed analysis of the rheological and dynamical characteristics indicate formation of a viscoelastic or elastoplastic zone (*16*)]. These processes result in deformations of the gold asperities, much beyond the elastic response regime.

For the case of near asperity overlap (Figs. 1B, 2, and 3), the gradually increasing confinement of the interasperity region is accompanied by the development of transient local stresses in front of the moving asperities (in Fig. 3 local stresses normal to the interfaces, τ_{zz}, and along the shear direction, τ_{xz}, are shown). Similar results were obtained for the overlapping-asperity case with even larger magnitudes of the stresses. The local shear and normal stresses that develop in the junction are of comparable magnitudes, with $\tau_{zz} > \tau_{xz}$ when the asperities come closer together (see t = 585 ps in Fig. 3). On exceeding a limiting value of close to 4 GPa, these accumulated local stresses lead to severe deformations and structural transformations of the asperities (*17*), mediated by the intervening lubricant molecules, even before the onset of direct intermetallic interactions (Figs. 1B, 2, and 3). In some locations along the asperity ridge (in the y direction), drainage of the lubricant molecules was complete when the sliding asperities passed over each other, leading to the formation of an intermetallic connective junction that sheared and eventually broke with continued sliding, resulting in the transfer of some metal atoms between the asperities. In this context we remark that in comparative simulations under the same conditions with no lubricant molecules in the junction, the magnitude of the interaction between the asperities and the degree of deformation were found to be insignificant. Furthermore, when the shearing process of the lubricated system was simulated with undeformable asperities, normal and tangential stresses in excess of 150 GPa developed, accompanied by trapping of a monolayer of alkane molecules between the asperities. This observation emphasizes that the dynamical mechanical response of the surfaces, and in particular, that of the nonuniform surface features (asperities), must be included for a proper description of the lubricated junction under these conditions.

Asperity deformations, complete lubricant drainage, growth of intermetallic junctions, shear-induced metal epitaxy, partial spreading by means of interlayer slip in the intermetallic junctions resulting in structural modifications of the surface topography (smoothing), and eventual rupture of such junctions are most pronounced for the case of overlapping asperities (Fig. 1C). The results for both this system and the near-overlap one suggest that in addition to the aforementioned lubricant-mediated smoothing of surface roughness, oscillatory shear or cyclic relative motion of the surfaces may lead to material fatigue, wear, and eventual failure due to repeated stress loading cycles of the surfaces.

For the near-overlap system, we comment also on the occurrence of local rupture, after asperities have collided, of the liquid film in the region between the departing asperities, resulting in the appearance of a nanometer-scale cavitated zone (*18*) (of a length scale of ~30 Å and lasting for a period of more than 100 ps). The appearance of such cavitated zones is associated with insufficient back-flow of lubricant molecules into that region. The formation and consequences of cavitated zones in lubricating films, which are subjects of basic and technological significance, have been recently discussed in the context of micro-EHL simulations (*19*) of film breakdown as two rough surfaces slide against each other.

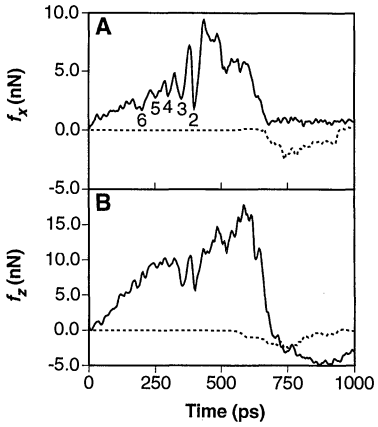

Fig. 2. (**A** and **B**) Total forces (in the x direction, f_x, and in the direction normal to the surfaces, f_z) on the gold solid surfaces from the alkane molecules (solid lines) plotted versus time for the near-overlap system (see Fig. 1B; for conversion to interasperity distances, see caption). Intermetallic forces between the opposing solid gold surfaces, with an onset on close approach of the asperities, are depicted by the dashed line. The numbers in f_x designate the "quantized" number of layers in the interasperity zone (see Fig. 1B). Note the correlation between the force oscillations and the structural variations in the lubricant.

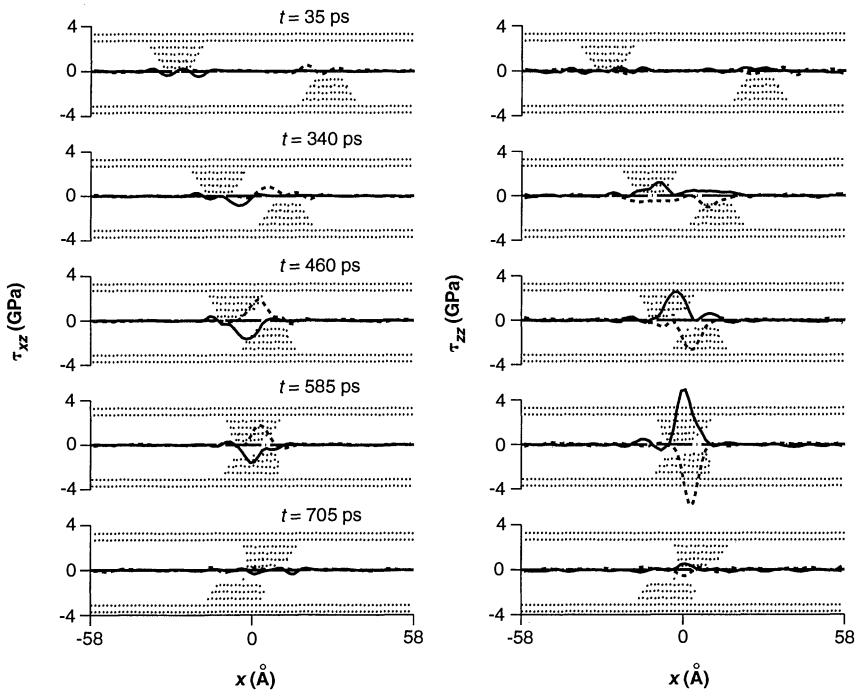

Fig. 3. Local stresses, exerted by the alkane molecules on the solid gold nonuniform substrates, plotted versus x. The stresses, obtained during a sliding simulation of the near-overlap system (see Fig. 1B), were calculated by averaging forces across the y direction. The solid and dashed lines denote the stresses on the solid top and bottom surfaces, respectively. Side views of the solid surfaces are superimposed, aiding in visualizing the relative interasperity configuration at the indicated times. Note the significant local stresses developing in front of the approaching asperities and the asperity deformations when the stresses achieve values of ~4 GPa.

Our findings provide insights into the atomic-scale fundamental processes of ultra-thin film lubrication, thus extending continuum EHL and micro-EHL treatments into the nanometer realm. Such investigations address some issues facing certain current novel technologies [such as high-density information storage and retrieval systems (*20*) and provide the impetus for future experimental and theoretical investigations.

REFERENCES AND NOTES

1. F. P. Bowden and D. Tabor, *Friction* (Anchor Press–Doubleday, Garden City, NY, 1973); *The Friction and Lubrication of Solids* (Clarendon, Oxford, 1950), part I; *ibid.* (Clarendon, Oxford, 1964), part II.
2. A. Cameron, *Principles of Lubrication* (Longman, London, 1966).
3. D. Dowson and G. R. Higginson, *Elastohydrodynamic Lubrication* (Pergamon, London, 1977).
4. R. Gohar, *Elastohydrodynamics* (Horwood, Chichester, England, 1988).
5. D. Dowson and V. Wright, Eds., *An Introduction to the Bio-Mechanics of Joints and Joint Replacements* (Mechanical Engineering, Edmunds, United Kingdom, 1978); see also (*11*), p. 485.
6. See review by D. Dowson, in *Fundamentals of Friction: Macroscopic and Microscopic Processes*, I. L. Singer and H. M. Pollock, Eds. (Kluwer, Dordrecht, Netherlands, 1992), p. 325.
7. See articles in (*6*); for a recent review, see B. Bhushan, J. N. Israelachvili, U. Landman, *Nature* **374**, 607 (1995).
8. U. Landman, R. N. Barnett, H.-P. Cheng, C. L. Cleveland, W. D. Luedtke, in *Computations for the Nano-Scale*, P. E. Bloch, C. Joachim, A. J. Fisher, Eds. (Kluwer, Dordrecht, Netherlands, 1993), p. 75; P. A. Thompson, M. O. Robbins, G. S. Grest, *ibid.*, p. 127.
9. See J. A. Greenwood in (*6*), p. 37 and p. 57.
10. S. M. Foiles, M. I. Baskes, M. S. Daw, *Phys. Rev. B* **33**, 7983 (1986).
11. J. P. Ryckaert and A. Bellemans, *Discuss. Faraday Soc.* **66**, 95 (1978).
12. T. K. Xia, J. Ouyang, M. W. Ribarsky, U. Landman, *Phys. Rev. Lett.* **69**, 1967 (1992).
13. U. Landman, W. D. Luedtke, J. Ouyang, T. K. Xia, *Jpn. J. Appl. Phys.* **32**, 1444 (1993).
14. M. P. Allen and D. J. Tildesley, *Computer Simulations of Liquids* (Clarendon, Oxford, 1987).
15. S. Granick, *Science* **253**, 1374 (1991).
16. J. Gao, W. D. Luedtke, U. Landman, *Langmuir*, in press.
17. It is of interest to note that a similar value for the yield pressure was obtained by us in previous studies of nanoindentation and elongation of gold [U. Landman, W. D. Luedtke, N. A. Burnham, R. J. Colton, *Science* **248**, 454 (1990); U. Landman and W. D. Luedtke, *J. Vacuum Sci. Technol. B* **9**, 414 (1991)]. This value is an order of magnitude larger than the yield stress of macroscopic gold samples, reflecting the plastic nature of the mechanical deformation in nanometer-scale metal structures.
18. U. Landman and W. D. Luedtke, *Mater. Res. Soc. Bull.* **17 (5)**, 36 (1993).
19. X. Ai, H. S. Cheng, L. Zheng, *ASME J. Tribol.* **115**, 102 (1993); L. Chang, A. Jackson, M. N. Webster, *Tribol. Trans.* **37**, 435 (1994).
20. B. Bhushan, *Tribology and Mechanics of Magnetic Storage Devices* (Springer, New York, 1990).

21. Supported by the U.S. Department of Energy, NSF, and the Air Force Office of Scientific Research. Computations were performed on CRAY Computers at the National Energy Research Supercomputer Center, Livermore, CA, at the Pittsburgh Supercomputing Center, and at the Georgia Institute of Technology Center for Computational Materials Science.

26 April 1995; accepted 29 August 1995

Imaging Pattern Formation in Surface Reactions from Ultrahigh Vacuum up to Atmospheric Pressures

H. H. Rotermund,* G. Haas, R. U. Franz, R. M. Tromp, G. Ertl

Two optical methods that allow pattern formation to be investigated at an arbitrary pressure are here applied to image concentration patterns of adsorbed species associated with heterogeneous catalytic reactions. In contrast to most surface physical techniques, these methods are not restricted to high vacuum conditions and thus bridge the "pressure gap." With carbon monoxide oxidation on a (110) surface of platinum as an example, the coupling mechanisms responsible for spatiotemporal self-organization in surface reactions were followed from reaction-diffusion control to the thermokinetic region, associated with phenomena not previously observed in pattern formation.

The applicability of most surface physical techniques is restricted to ambient gas pressures below about 10^{-3} mbar. This gives rise to a "pressure gap" between model studies conducted at low pressures and the conditions of "real" catalysis. Data measured at low pressures exploring the mechanism and kinetics of a heterogeneously catalyzed reaction can be theoretically extrapolated across a large pressure range (*1*); however, there are also cases in which the phenomena occurring on opposite sides of this gap are different in nature. This is the case for nonlinear effects causing spatiotemporal pattern formation on a reacting surface (*2*): At low pressures the conditions are nearly isothermal, and concentration patterns are formed by coupling of the reaction and surface diffusion. Phenomena of this type have been widely studied with the recently developed technique of photoemission electron microscopy (PEEM) (*3–5*). At higher pressures, on the other hand, finite temperature differences caused by variations of the heat release associated with the reaction give rise to thermokinetic waves governed by the heat conductance of the system, which to date have been imaged primarily by techniques based on infrared emission (*6*).

In this report we demonstrate how two optical methods may be used to image surface patterns at arbitrary pressure. With these techniques, the continuous range of coupling mechanisms responsible for spatiotemporal self-organization in surface reactions (for example, diffusion and heat conductance) becomes accessible to experimental investigation. The two techniques, ellipsomicroscopy for surface imaging (EMSI) and reflection anisotropy microscopy (RAM), are closely related and are based on changes of the degree of polarization of light reflected from a surface.

The EMSI technique is based on ellipsometry, which is well-established and has been used as an imaging method for characterizing structures on surfaces with thick-

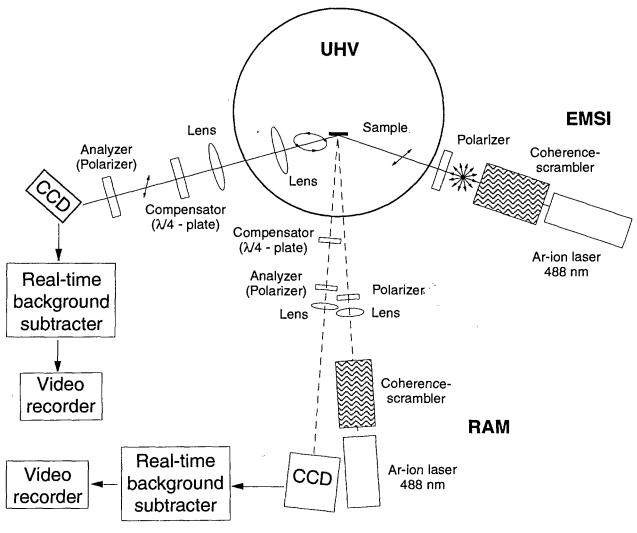

Fig. 1. Experimental setup for EMSI and RAM. Light from an Ar-ion laser (wavelength $\lambda = 488$ nm, power = 100 mW) is reduced in coherence as it passes through a vibrating multimode optical fiber; it is then linearly polarized and illuminates the surface at an angle of 70° with respect to its normal for EMSI (solid path) and close to normal incidence for RAM (dashed path). After reflection, the beam is imaged onto a charge-coupled device (CCD) chip by lenses (enabling magnifications between ×1 and ×50), after passing through a compensator ($\lambda/4$ plate) and being adjusted close to zero intensity by the analyzer. An image processor (Hamamatsu Argus 20) permits background subtraction in real time. Arrows indicate the polarization of the light for EMSI.